Research Article

Agnieszka Sienkiewicz, Ewelina Kusiak-Nejman*, Agnieszka Wanag*, Konstantinos Aidinis, Danuta Piwowarska, Antoni W. Morawski, and Niko Guskos

High-temperature treated TiO_2 modified with 3-aminopropyltriethoxysilane as photoactive nanomaterials

https://doi.org/10.1515/rams-2022-0264
received April 27, 2022; accepted August 09, 2022

Abstract: A series of titanium dioxide (TiO_2) modified with 3-aminopropyltriethoxysilane (APTES) was prepared by high-temperature calcination in an argon atmosphere in the temperature range from 800 to 1,000°C. The properties of the obtained samples were compared with those of pure TiO_2 annealed under the same conditions. Examining electron paramagnetic resonance (EPR) parameters at room temperature for APTES–TiO_2 showed an intense resonance line from defects related to conducting electrons with g_{eff} from 2.0028 to 2.0026 and 1.9052 for temperatures 800, 900, and 1,000°C, respectively, while for pure calcined TiO_2, these ERP lines were not observed. With the increase in the calcination temperature to 900°C for APTES–TiO_2 samples, the EPR increases linearly. This has been combined with a relatively high anatase content and small crystallites. The EPR line intensity at RT calculated for 1 g of sample showed an almost linear relationship with the photoactivity in removing ORANGE II dyes from water.

Keywords: APTES-modified TiO, photoactivity, EPR measurements

*** Corresponding author: Ewelina Kusiak-Nejman,** Department of Inorganic Chemical Technology and Environment Engineering, Faculty of Chemical Technology and Engineering, West Pomeranian University of Technology in Szczecin, Pułaskiego 10, 70-322 Szczecin, Poland, e-mail: ewelina.kusiak@zut.edu.pl
*** Corresponding author: Agnieszka Wanag,** Department of Inorganic Chemical Technology and Environment Engineering, Faculty of Chemical Technology and Engineering, West Pomeranian University of Technology in Szczecin, Pułaskiego 10, 70-322 Szczecin, Poland, e-mail: agnieszka.wanag@zut.edu.pl
Agnieszka Sienkiewicz: Department of Inorganic Chemical Technology and Environment Engineering, Faculty of Chemical Technology and Engineering, West Pomeranian University of Technology in Szczecin, Pułaskiego 10, 70-322 Szczecin, Poland, e-mail: agnieszka.sienkiewicz@zut.edu.pl
Konstantinos Aidinis: Department of Electrical Engineering, Ajman University of Science and Technology, PO Box 346, Ajman, United Arab Emirates, e-mail: k.aidinis@ajman.ac.ae
Danuta Piwowarska: Department of Technical Physics, West Pomeranian University of Technology in Szczecin, Al Piastów 17, 70-310 Szczecin, Poland, e-mail: danuta.piwowarska@edu.zut.pl
Antoni W. Morawski: Department of Inorganic Chemical Technology and Environment Engineering, Faculty of Chemical Technology and Engineering, West Pomeranian University of Technology in Szczecin, Pułaskiego 10, 70-322 Szczecin, Poland, e-mail: antoni.morawski@zut.edu.pl
Niko Guskos: Department of Technical Physics, West Pomeranian University of Technology in Szczecin, Al Piastów 17, 70-310 Szczecin, Poland, e-mail: nguskos@edu.zut.pl

1 Introduction

Titanium dioxide (TiO_2), a wide band gap inorganic semiconductor (3.23 eV for the most active anatase phase), is a fascinating material from the perspective of both pure theoretical science and industrial use [1]. Its extensive application in various fields, particularly in heterogeneous photocatalysis [2–4]. Because TiO_2 is an inexpensive, stable, and non-toxic material, the significant efforts made over the past decades in the synthesis of modified TiO_2 have provided nanomaterials with new properties and applications with greatly enhanced performance [5–8].

Modified TiO_2 has been and continues to be studied by magnetic resonance for years [9–12]. Electron paramagnetic resonance (EPR) is a spectroscopic method frequently utilized to investigate the structure and interactions of paramagnetic entities like transition metal ions, free radicals, and defects in solids such as electrons trapped in lattice vacancies [13]. These defects are important for the TiO_2 photocatalytic properties [13,14]. Information from the EPR study supplements data from other characterization methods and gives a more detailed picture of the surface and interfacial electron transfer processes [14]. In TiO_2-based photocatalysts, the photogenerated charges like electrons (e^-) and holes (h^+) have sufficiently distinct structures and electron configurations to enable the spectral

resolution of each species. Additionally, the structural diversity between anatase and rutile phases makes it possible to observe electrons trapped in each of the two TiO_2 polymorphous forms. Such sensitivity to the structural geometry of the trapping sites results in EPR being a beneficial technique for studying electron transfer processes in photocatalysts [14,15] and confirming the paramagnetic reactive species formation in studied materials [16,17]. It is a fairly known fact that silicon and its oxides can significantly modify the surface of TiO_2. For example, the pronounced reversible surface change of the hydrophilic-to-hydrophobic for TiO_2/Si coatings is described [18]. Recently, the narrow EPR signal intensity with the temperature decrease is observed. This effect is explained by the Anderson localization of conduction electrons in the defected crystalline structure of rGO [19].

In our previous studies, a series of materials based on TiO_2 modified with 3-aminopropyltriethoxysilane (APTES) with improved photocatalytic activity under artificial solar light (ASL) irradiation were successfully synthesized [20]. The new photocatalysts were prepared in a two-step process by a 4-hour solvothermal functionalization in a pressure autoclave at 180°C and calcination in an argon atmosphere in the temperature range from 800 to 1,000°C, where the modifier concentrations were 100, 500 and 1,000 mM. The presence of APTES after modification was confirmed via FT-IR/DRS measurements and the EDX mapping and N, C, and Si content analysis. It was reported that the presence of carbon and silicon in the APTES/TiO_2 samples contributed to an effective delay in the phase transformation of the anatase to rutile, the increase in crystallite size (during annealing) affected the decrease in specific surface area. The efficiency of the prepared materials was studied during the methylene blue (MB) decomposition under ASL irradiation. The calcination enhanced the ASL-driven photocatalytic activity of all APTES-modified TiO_2. It was noted that the highest dye decomposition degree was obtained for materials annealed at 900°C. Moreover, considering the highest performance and economic aspects, TiO_2–4 h–180°C–500 mM–Ar–900°C was found to be the most prospective nanomaterial. The most important conclusion was the experimental finding that in the modified APTES/TiO_2 samples during calcination to 900°C, the anatase phase is still present in an amount of up to 96% with crystallite size of 30 nm, while the rutile phase with crystallite size of 55 nm occurred with a slight increase of about 6% [20].

In the present study, we extended our previous work and, for the first time, used EPR to study the magnetic properties of a selected series of APTES/TiO_2 nanomaterials functionalized with 500 mM of modifier annealed in an argon atmosphere. The photocatalysts modified with 500 mM of APTES were chosen for EPR studies because they exhibited higher photoactivity than the materials functionalized with 100 and 1,000 mM concentrations. To the best of our knowledge, this is the first publication presenting results from EPR studies of APTES-modified TiO_2 photocatalysts heated at high temperatures, which have photoactivity in the ASL range. Furthermore, in this article, we also extended our previous studies by adding activity results for Orange II under both ultraviolet (UV) light and ASL irradiation. EPR measurements were made at room temperature because photocatalytic activation was performed at this temperature.

It is interesting to compare the formation of magnetic moments and their intensity concerning the photoactivity and determine whether they increase photoactivity in the TiO_2 samples modified with APTES after calcination.

2 Experimental

The crude TiO_2 slurry, provided by the chemical plant Grupa Azoty Zakłady Chemiczne "Police" S.A. (Police, Poland), was used as a TiO_2 starting material. APTES utilized as a silicon precursor was purchased from Merck KGaA (Darmstadt, Germany). Ethanol from P.P.H. "STANLAB" Sp.J., (96%, Poland) was used as a solvent of APTES. Orange II ($C_{16}H_{11}N_2NaO_4S$, ≥85%, Firma Chempur®, Poland) was used as a model for organic water pollution. The APTES-modified TiO_2 nanomaterials were obtained using the solvothermal method and calcination process. The concentration of the APTES in ethanol was 500 mM. The samples were calcined at 800, 900, and 1,000°C for 4 h in Ar atmosphere (60 mL·min^{-1}, purity of 5.0, and Messer Polska Sp. z o.o., Poland). The procedure is described in detail in our previous publication [20].

2.1 Photocatalytic activity measurements

The Orange II decomposition processes under ASL irradiation with the intensity of 837 W·m^{-2} for 300–2,800 nm and 0.3 W·m^{-2} for the 280–400 nm regions as well as under UV–Vis light irradiation, with the radiation intensity of 65 W·m^{-2} for 300–2,800 nm and 36 W·m^{-2} for the 280–400 nm region, were carried out to determine the photoactivity of the prepared materials. The experiments were conducted in a glass beaker using 0.5 L of dye solution with an initial concentration of 5 mg·L^{-1} and 0.5 g·L^{-1} of the appropriate photocatalyst. Before irradiation,

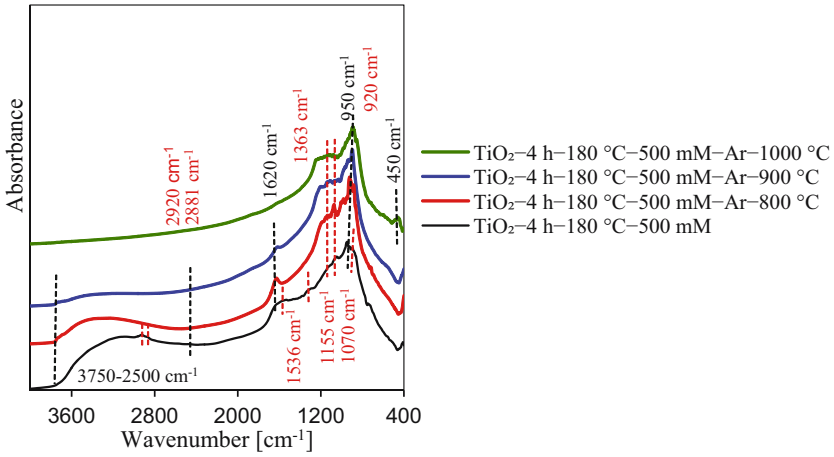

Figure 1: Diffuse reflectance Fourier transform infrared spectra of APTES/TiO_2 nanomaterials [20].

adsorption measurements were performed in light-free conditions for 60 min to establish the adsorption–desorption equilibrium at the photocatalyst–dye interface. After that, the suspension was subjected to ASL radiation. The Orange II concentration was analyzed every 60 minutes using the V-630 UV–Vis spectrometer (JASCO International Co., Japan). The obtained activity results were converted as the mass of MB or Orange II removed per 1 g of photocatalyst.

3 Results and discussion

Several new characteristic bands from APTES were noted in the spectra presented in Figure 1, indicating that the synthesis of the new nanomaterials method was carried out successfully. These bands are located at about 2,920, 2,881, 1,536, 1,363, 1,155, and 1,070 cm^{-1} and assigned to the symmetric and asymmetric stretching vibration of alkyl groups, the asymmetric $-NH_3^+$ deformation modes, C–N bonds Si–O–Si stretching vibrations, and Si–O–C stretching mode, respectively. The stretching vibrations of Ti–O–Si bonds are observed between 950 and 910 cm^{-1}. However, the band at 910 cm^{-1} is related to the condensation reaction that occurred between silanol and surface –OH groups [20]. It should be noted that after calcination, some characteristic bands for APTES such as alkyl groups, $-NH_3^+$ and C–N bonds did not present. The reason for this was the non-permanent bond between these groups and the TiO_2 surface. The presence of APTES on the TiO_2 surface, and thus, the effectiveness of the modification was confirmed also by nitrogen and carbon analysis and EDX mapping presented in our previous article [20]. It was found that the addition of silicon and carbon in APTES/TiO_2 samples effectively delayed the anatase-to-rutile phase transformation and the increase in crystallite size of both TiO_2 polymorphous forms during high-temperature annealing. Therefore, the calcined APTES-functionalized TiO_2 showed higher specific surface area and pore volume values than the reference materials (Table 1). Furthermore, the modified TiO_2 surface charge change from positive to negative after calcination enhanced the dye adsorption degree [20]. EDS measurements show that silicon content fluctuates around 2% for all calcined samples by mass with carbon content from 0.17 to 0.08 and 0.03 wt% for temperatures 800, 900, and 1,000°C, respectively.

For pure starting-TiO_2 samples calcined only in argon at 800, 900, and 1,000°C and without APTES modification (TiO_2–Ar–800°C, TiO_2–Ar–900°C, and TiO_2–Ar–1000°C, that contain only rutile with crystallites above 100 nm [20]), the spectral spectra measurements did not show any EPR signal at RT in the investigated measuring range.

Contrary to the above-mentioned samples, during calcination in argon at 800, 900, and 1,000°C with APTES modification (TiO_2–4 h–180°C–500 mM–800°C, TiO_2–4 h–180°C–500 mM–900°C, and TiO_2–4 h–180°C–500 mM–1000°C), an intense symmetrical resonance line appeared. In Figure 2 are given experimental EPR spectra measured at RT compared to the uncalcined TiO_2–4 h–180°C–500 mM material. For EPR parameters, calculation spectra have been collected, as shown in Figure 3.

The EPR parameters: effective g-factor (g_{eff}), peak-to-peak linewidth ΔBpp, and integrated intensity I_{int} can be calculated from the magnetic resonance condition: $h\nu = g_{eff}\,\mu_B B_r$ where h is Planck constant, ν – the microwave frequency, μ_B – Bohr magneton, and B_r magnetic

Table 1: Physicochemical properties of starting-TiO_2, reference samples, and APTES-modified TiO_2 nanomaterials [20]

Sample name	S_{BET} ($m^2 \cdot g^{-1}$)	V_{total} ($cm^3 \cdot g^{-1}$)	Anatase in crystallite phase (%)	Anatase crystallite size (nm)	Rutile in crystallite phase (%)	Rutile crystallite size (nm)	Zeta potential δ (mV)
TiO_2–Ar–800°C	6	0.020	1	>100	99	>100	−35.9
TiO_2–Ar–900°C	3	0.008	—	—	100	>100	−36.7
TiO_2–Ar–1,000°C	4	0.009	—	—	100	>100	−41.3
TiO_2–4 h–180°C–500 mM	124	0.162	96	15	4	48	+22.8
TiO_2–4 h–180°C–500 mM–800°C	95	0.221	96	20	4	58	−47.4
TiO_2–4 h–180°C–500 mM–900°C	46	0.192	94	30	6	55	−51.0
TiO_2–4 h–180°C–500 mM–1000°C	16	0.069	12	47	88	>100	−41.3

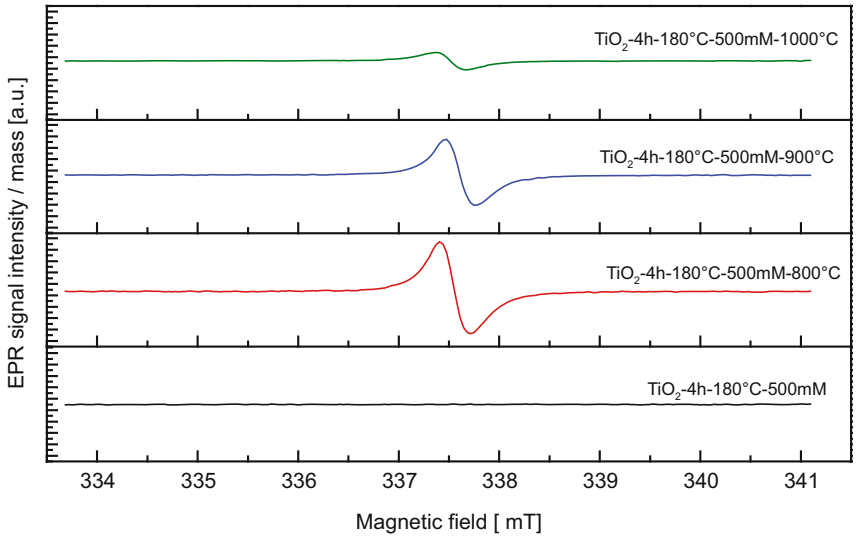

Figure 2: EPR spectra measured at RT of the uncalcined TiO_2–4 h–180°C–500 mM, and annealed TiO_2–4 h–180°C–500 mM–800°C, TiO_2–4 h–180°C–500 mM–900°C, and TiO_2–4 h–180°C–500 mM–1000°C. The spectra are rescaled to a unit mass.

resonance field. The integrated intensity, proportional to the magnetic susceptibility on microwave frequency of a spin system producing EPR spectrum, is defined as $I_{int} = A \cdot \Delta Bpp$ where A is signal amplitude. At high temperatures, the width of the resonance lines decreases significantly with a change in calcination temperature. So that the relaxation processes depend on the temperature of calcination, as given in Table 2.

According to the data listed in Table 2, all parameters (effective g-factor (g_{eff}), signal amplitude A, and integrated intensity I_{int}) decrease with increased temperature from 800 to 1,000°C, whereas peak-to-peak linewidth ΔBpp shows independent changes from temperature with their fittings by Lorentzian function.

A step-by-step change in the g_{eff} value of the parameter for a nanocomposite calcined at temperatures of 800–1,000°C may be caused by a change in the resonance

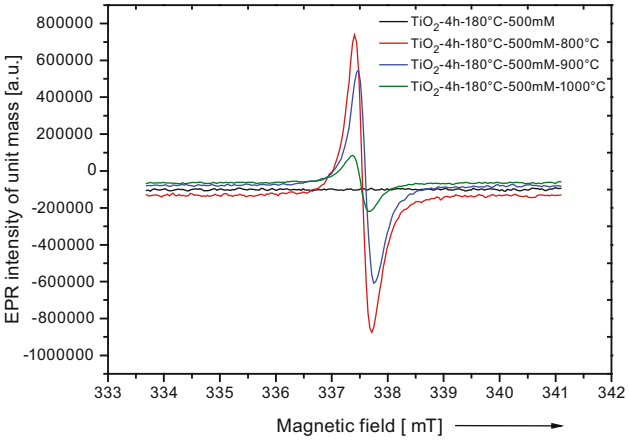

Figure 3: EPR spectra at RT of the uncalcined TiO_2–4 h–180°C–500 mM, and annealed TiO_2–4 h–180°C–500 mM–800°C, TiO_2–4 h–180°C–500 mM–900°C and TiO_2–4 h–180°C–500 mM–1000°C with their simulations.

Table 2: EPR parameters for measurements at RT for studied samples

EPR Parameters	*A* (a.u.)	Δ*B*pp (mT)	I_{int} (mT^2)	g_{eff}
TiO_2–4 h–180°C–500 mM–800°C	870242.5406	0.28770	7.2031×10^4	2.0028
TiO_2–4 h–180°C–500 mM–900°C	622752.3100	0.28086	4.9124×10^4	2.0026
TiO_2–4 h–180°C–500 mM–1000°C	150861.3207	0.30198	1.3757×10^4	1.9052

Table 3: Summary of the EPR signal intensity in studied samples per 1 g

Sample name	EPR intensity line/1 g of photocatalyst
TiO_2–Ar–800°C	0
TiO_2–Ar–900°C	0
TiO_2–Ar–1000°C	0
TiO_2–4 h–180°C–500 mM	0
TiO_2–4 h–180°C–500 mM–800°C	65,796
TiO_2–4 h–180°C–500 mM–900°C	46,632
TiO_2–4 h–180°C–500 mM–1000°C	13,922

condition by forming an additional internal magnetic field. It can be formed by the resulting magnetic agglomerates, reducing its intensity. Observed diminishing energy gape E_g from 3.27 eV to 3.21 and 3.02 confirm changes of electron behavior [20].

These EPR parameters at the temperatures of 800, 900, and 1,000°C correlate well with the corresponding decrease in the content of anatase from 94 to 12 wt% and the increase in the size of their crystallites from 20 through 30 to 47 nm. An increase in the rutile content from 4 to 88 wt% and an increase in the size of rutile crystallites from 58 to over 100 nm, at appropriate temperatures [20], were also noticed.

Table 4: Summary of photoactivity for Orange II decomposition under UV and ASL radiations and the intensity of the EPR signal line per gram of calcined APTES/TiO_2 photocatalysts

Sample name	Amount of removed dye after 360 min of ASL irradiation (mg of Orange II/1 g of photocatalyst)	Amount of removed dye after 180 min of UV irradiation (mg of Orange II/1 g of photocatalyst)	EPR intensity line/1 g of photocatalyst
TiO_2–4 h–180°C–500 mM	0.0	0.0	0
TiO_2–4 h–180°C–500 mM–800°C	1.7	28.2	65,796
TiO_2–4 h–180°C–500 mM–900°C	1.2	25.8	46,632
TiO_2–4 h–180°C–500 mM–1000°C	0.2	6.3	13,922

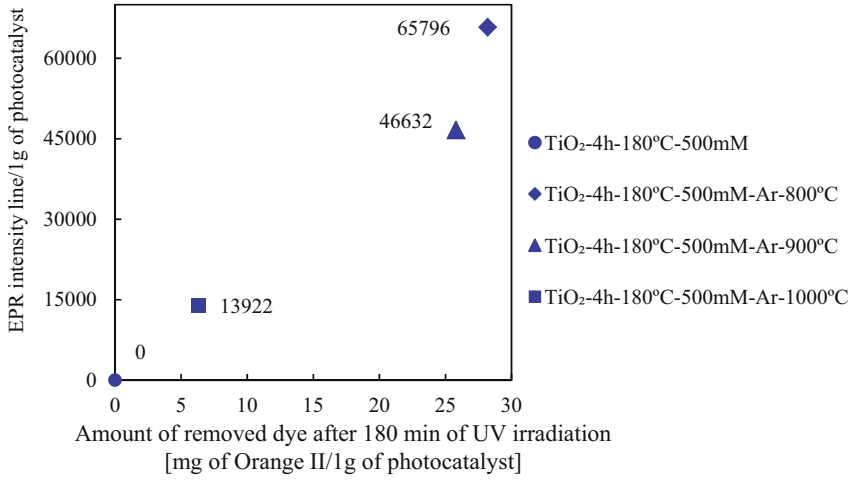

Figure 4: Correlation between the amount of Orange II dye removed after 180 min of UV irradiation and EPR line intensity for APTES/TiO_2 nanomaterials.

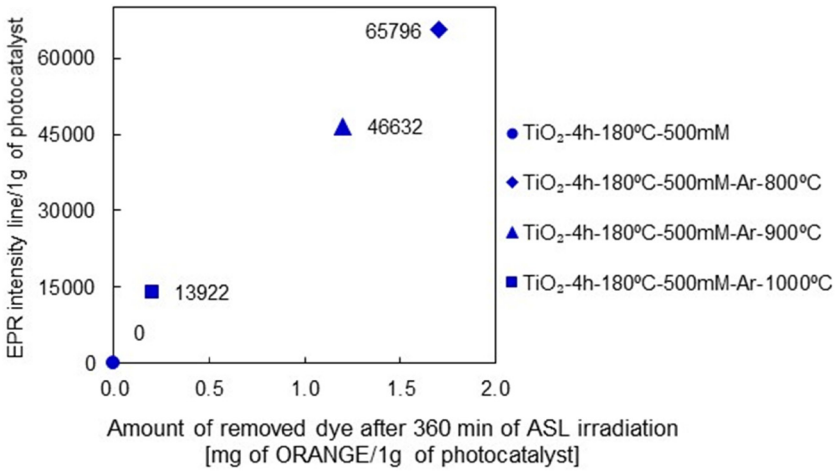

Figure 5: Correlation between the amount of Orange II dye removed after 360 min of ASL irradiation and EPR line intensity for APTES/TiO_2 nanomaterials.

Additionally, the observed EPR signal has recently been associated with conduction electrons [21] but a similar signal also occurs from oxygen defects. Both are related to electron transfer. High calcination temperatures can significantly improve photocatalytic properties. In both cases, electron transfer plays an important role. In the first case, at room temperature, the EPR signal is more intense. Rather, this signal comes from the total area of the nanocomposite. Surface effects also play an important role in photocatalytic processes.

Table 3 summarizes the obtained intensities of calcined samples with and without APTES addition, converted to 1 g of photocatalyst. As can be seen, the samples without modifier showed no EPR signal, while the samples supplemented with APTES exhibited intense EPR at RT lines. The calcined samples without the addition of silicon showing no EPR lineage were also photocatalytically inactive, except for the degradation of the Orange II dye in the UV range, where small activities were recorded. Therefore, the EPR lines and the photocatalytic activities of these samples in the scope of UV and ASL radiation during the degradation of dyes, Orange II, are summarized in Table 4.

For Orange II, these samples, without APTES modification and calcination, showed no activity in both UV and ASL ranges.

It can be seen that the intensity of the photocatalytic decomposition of the Orange II dye, both in UV and in ASL radiation (Figures 4 and 5), is linearly related to the intensity of the EPR at the RT line signal, with the highest activity and intensity of the EPR line achieved by the sample calcined at 800°C.

It was mentioned earlier that the obtained partially reduced graphene oxide (prGO) has EPR spectra on the broad and narrow lines [22]. The resonance line was attributed to the conduction electrons. A similar resonance line was obtained in the samples discussed herein, with a more intense one for the nanocomposite modifications of APTES–TiO_2.

It is well known the importance of electron transfer, especially in the temperature range above 650–700°C, as they cause significant changes in modified TiO_2 nanocomposites photocatalytic processes. With the right concentration of conduction electrons, maximum photocatalytic efficiency is obtained. In the modified APTES–TiO_2, it was possible to obtain larger active surfaces [20]. Hence, at room temperature, we have found more localized magnetic defects informing about the increase in conduction electrons similar to postulated for hydrothermally reduced graphene oxide [19].

4 Conclusions

Modified APTES–TiO_2 nanocomposites after calcination in an argon atmosphere at temperatures 800, 900, and 1,000°C showed changes within many properties compared to pure calcined TiO_2 that strongly depend on the temperature of annealing. New EPR lines appeared in calcined APTES–TiO_2 materials, whereas these lines were absent for pure TiO_2. EPR studies at room temperature for calcined APTES–TiO_2 have shown the formation of a high concentration of defects associated with conduction electrons that strongly depend on the calcination temperature – g_{eff} decreased from 2.0028 to 2.0026 and 1.9052 for 800, 900, and 1,000°C, respectively. At an

annealing temperature of 1,000°C, concentration decreases significantly. It is probably the result of the formation of magnetic agglomerates. The EPR line intensity at RT calculated for 1 g of sample showed an almost linear relationship with the photoactivity in removing Orange II dyes from water.

Acknowledgment: This work was supported by grant 2017/27/B/ST8/02007 from the National Science Centre, Poland.

Funding Information: This research was funded by the grant 2017/27/B/ST8/02007 from the National Science Centre, Poland.

Author contributions: A. Sienkiewicz, A. Wanag, E. Kusiak-Nejman: methodology, conceptualization, writing – original draft, K. Aidinis: software, validation. D. Piwowarska: EPR measurements and their development, A.W. Morawski: visualization, conceptualization, writing – original draft, supervision, funding acquisition, N. Guskos: visualization, conceptualization, writing – original draft, supervision.

Conflict of interest: The authors declare that they have no known competing financial interests or personal relationships that could have appeared to influence the work reported in this study.

Data availability statement: All data generated or analyzed during this study are included in this published article or are available from the corresponding author on reasonable request.

References

[1] Wan, L., J. F. Li, J. Y. Feng, W. Sun, and Z. Q. Mao. Anatase TiO_2 films with 2.2eV band gap prepared by micro-arc oxidation. *Materials Science and Engineering: B*, Vol. 139, 2007, pp. 216–220.

[2] He, J., A. Kumar, M. Khan, and I. M. C. Lo. Critical review of photocatalytic disinfection of bacteria: from noble metals- and carbon nanomaterials-TiO_2 composites to challenges of water characteristics and strategic solutions. *Science of the Total Environment*, Vol. 758, 2021, id. 143953.

[3] Jiang, D., T. A. Otitoju, Y. Ouyang, N. F. Shoparwe, S. Wang, A. Zhang, and S. Li. A review on metal ions modified TiO_2 for photocatalytic degradation of organic pollutants. *Catalysts*, Vol. 11, 2021, id. 1039.

[4] Li, Z., Z. Li, C. Zuo, and X. Fang. Application of nanostructured TiO_2 in UV photodetectors: A review. *Advanced Materials*, Vol. 34, No. 28, 2022, id. 2109083.

[5] Hou, X., K. Aitola, and P. D. Lund. TiO_2 nanotubes for dye-sensitized solar cells – A review. *Energy Science & Engineering*, Vol. 9, 2021, pp. 921–937.

[6] Al Zoubi, W., A. A. S. Al-Hamdani, S. Sunghun, and Y. G. Ko. A review on TiO_2-based composites for superior photocatalytic activity. *Reviews in Inorganic Chemistry*, Vol. 41, No. 4, 2021, pp. 213–222.

[7] Maheswari, P., S. Harish, M. Navaneethan, C. Muthamizhchelvan, S. Ponnusamy, and Y. Hayakawa. Bio-modified TiO_2 nanoparticles with Withania somnifera, Eclipta prostrata and Glycyrrhiza glabra for anticancer and antibacterial applications. *Materials Science and Engineering: C*, Vol. 108, 2020, id. 110457.

[8] Sienkiewicz, A., A. Wanag, E. Kusiak-Nejman, E. Ekiert, P. Rokicka-Konieczna, and A. W. Morawski. Effect of calcination on the photocatalytic activity and stability of TiO_2 photocatalysts modified with APTES. *Journal of Environmental Chemical Engineering*, Vol. 9, 2021, id. 104794.

[9] Coronado, J. M., A. J. Maira, L. C. Conesa, K. L. Yeung, V. Augugliaro, and J. Soria. EPR study of the surface characteristics of nanostructured TiO_2 under UV irradiation. *Langmuir*, Vol. 17, 2001, pp. 5368–5374.

[10] Kumar, C. P., N. O. Gopal, T. C. Wang, M. S. Wong, and S. C. Ke. EPR investigation of TiO_2 nanoparticles with temperature-dependent properties. *The Journal of Physical Chemistry B*, Vol. 110, 2006, pp. 5223–5229.

[11] Dimitrijevic, N. M., Z. V. Saponjic, B. M. Rabatic, O. G. Poluektov, and T. Rajh. Effect of size and shape of nanocrystalline TiO_2 on photogenerated charges. An EPR study. *The Journal of Physical Chemistry C*, Vol. 111, No. 40, 2007, pp. 14597–14601.

[12] Konovalova, T. A., L. D. Kispert, and V. V. Konovalov. Surface modification of TiO_2 nanoparticles with carotenoids. EPR study. *The Journal of Physical Chemistry B*, Vol. 103, 1999, pp. 4672–4677.

[13] Typek, J., N. Guskos, G. Zolnierkiewicz, M. Pilarska, A. Guskos, E. Kusiak-Nejman, and A.W. Morawski. Magnetic properties of TiO_2/graphitic carbon nanocomposites. *Reviews on Advanced Materials Science*, Vol. 58, 2019, pp. 107–122.

[14] Hurum, D. C., A. G. Agrios, S. E. Crist, K. A. Gray, T. Rajh, and M. C. Thurnauer. Probing reaction mechanisms in mixed phase TiO_2 by EPR. *Journal of Electron Spectroscopy and Related Phenomena*, Vol. 500, 2006, pp. 155–163.

[15] Dvoranová, D., M. Mazúr, I. Papailias, T. Giannakopoulou, C. Trapalis, and V. Brezová. EPR investigations of G-C_3N_4/TiO_2 nanocomposites. *Catalysts*, Vol. 8, 2018, id. 47.

[16] Barbierikova, Z., D. Dvoranova, V. Brezova, E. Dzunuzowic, D. N. Sredojevc, V. Lazic, and J.M. Nedeljkovic. Visible-light-responsive surface-modified TiO_2 powder with 4-chlorophenol: A combined experimental and DFT study. *Optical Materials*, Vol. 89, 2019, pp. 237–242.

[17] Barierkova, Z., E. Plizingrova, M. Motlochova, P. Bezdicka, J. Bohacek, D. Dvoranowa, et al. V. N-Doped titanium dioxide nanosheets: Preparation, characterization and UV/visible-light activity. *Applied Catalysis B: Environmental*, Vol. 232, 2018, pp. 397–408.

[18] Rudakova, A. V., A. V. Emeline, A. I. Romanychev, and D. W. Bahnemann. Photoinduced hydrophobic behavior of TiO_2 thin film on Si substrate. *Journal of Alloys and Compounds*, Vol. 872, 2021, id. 159746.

[19] Augustyniak-Jabłokow, M. A., R. Strzelczyk, and R. Fedaruk. Localization of conduction electrons in hydrothermally reduced graphene oxide: electron paramagnetic resonance studies. *Carbon*, Vol. 168, 2020, pp. 665–672.

[20] Sienkiewicz, A., P. Rokicka-Konieczna, A. Wanag, E. Kusiak-Nejman, and A. W. Morawski. Artificial solar light-driven APTES/TiO_2 photocatalysts for methylene blue removal from water. *Molecules*, Vol. 27, 2022, id. 947.
[21] Augustyniak-Jabłkow, M. A., R. Strzelczyk, and R. Fedaruk. Localization of conduction electrons in hydrothermally reduced graphene oxide: Electron paramagnetic resonance studies. *Carbon*, Vol. 168, 2020, pp. 665–672. doi: 10.1016/j.carbon.2020.07.023.
[22] Guskos, N., G. Zolnierkiewicz, A. Guskos, K. Aidinis, A. Wanag, E. Kusiak-Nejman, et al. Magnetic moment centers in titanium dioxide photocatalysts loaded on reduced graphene oxide flakes. *Reviews on Advanced Materials Science*, Vol. 60, 2021, pp. 57–63.